



Research paper

Highly selective hydrazone based reversible colorimetric chemosensors for expeditious detection of CN^- in aqueous media

Jahangir Mondal, Amit Kumar Manna, Goutam K. Patra*

Department of Chemistry, Guru Ghasidas Vishwavidyalaya, Bilaspur (C.G.), India

ARTICLE INFO

Article history:

Received 30 October 2017

Received in revised form 12 January 2018

Accepted 15 January 2018

Keywords:

Schiff base

Hydrazones

Colorimetric sensor

 CN^- sensor

Reversible sensor

ABSTRACT

Herein we have described the design and syntheses of two novel hydrazone based N, O donor Schiff-base colorimetric sensors L_1 and L_2 for selective sensing of cyanide ions in 2:1 $\text{CH}_3\text{CN-H}_2\text{O}$ mixture. L_1 and L_2 have been characterized by ^1H NMR, IR spectroscopy, HRMS spectrometry and elemental analyses. Interactions of L_1 and L_2 with CN^- provide remarkable color change from yellow to red (for L_1) and yellow to pink (for L_2) along with change in the absorption maxima, enabling naked-eye sensing of CN^- ion, without use of any expensive equipment. From the job's plot analyses, HRMS spectral studies and ^1H NMR analyses, 1:1 binding stoichiometry of chemosensor L_1 and 1:2 binding stoichiometry of chemosensor L_2 towards cyanide ion have been confirmed. The detection limits reach up to 1.3 μM for L_1 and 1.0 μM for L_2 which are lower than the maximum permissible level of CN^- in drinking water set by WHO. The other competitive anions (OAc^- , F^- , Cl^- , Br^- , I^- , H_2PO_4^- , NO_2^- , NO_3^- , HSO_4^- , N_3^- , CO_3^{2-} , PO_4^{3-} , S^{2-} , and BO_3^{3-}) showed very negligible interference for detection of cyanide at that concentration level. The sensing mechanism has further been confirmed by DFT studies. Both the chemosensors L_1 and L_2 have been successfully applied for the determination of CN^- ions in real water samples and simulated urine samples.

© 2018 Elsevier B.V. All rights reserved.

1. Introduction

The development of chemosensors for anions has become a subject of intense research interest, because anions play important roles in a wide range of environmental, clinical, chemical, and biological applications [1–5]. Among the various anions, cyanide is one of the maximum concerned, because it is one of the most rapidly acting and powerful poisons. Its toxicity results from its propensity to bind to the iron in cytochrome c oxidase, interfering with electron transport and resulting in hypoxia [6–11]. Cyanide could be absorbed through the lungs, gastrointestinal tract and skin, leading to vomiting, convulsion, loss of consciousness, and eventual death [12–14]. In spite of its toxicity, its application in various areas as raw material for synthetic fibers, resins, herbicides, and the gold extraction process is unavoidable [15–17], which releases cyanide into the environment as a toxic contaminant. Thus, there is a need for an effective sensing system to monitor cyanide concentration from pollutant sources. Among various approaches such as fluorescence techniques and electrochemical methods for the detection of cyanide, the most attractive approach

focuses on novel colorimetric cyanide sensors, which allow naked-eye detection of the color change without resorting to the use of expensive instruments [18–21]. Colorimetric materials have advantages such as low cost, a rapid response rate, easy detection and high selectivity [22–26]. Therefore, colorimetric sensors that are capable of recognizing cyanide in an aqueous environment are of current interest.

Hydrazone derivatives form an important class of most widely used organic compounds and have versatile applications in various advanced fields including the ink jet printing [27], pigments [28], photography [29], molecular recognition [30], multidentate ligands [31] and fluorescent materials [32]. These are also found to be significant due to their extensive applications in pharmaceutical and biological activities like anticancer, anti-inflammatory, antibacterial, antifungal, antimalarial, antitubercular activities [33], and potential inhibitor for various enzymes [34]. Hydrazones containing chromophoric group like nitro are having hydrogen donor capability and are reported as good anion receptors [35,36]. The success of hydrazone derivatives is also due to the simplicity of their synthesis, to the many possibilities presented by variation of the diazo compounds and coupling components, the generally high molar extinction coefficient as well as to the good light and wet fastness properties [37]. Although many optical

* Corresponding author.

E-mail address: patra29in@yahoo.co.in (G.K. Patra).

sensors for cyanide detection have been reported based on H-bonding interaction [38], nucleophilic addition reaction [39], metal complex displacement approach [40], most of them suffer from various limitations such as lengthy synthetic protocol, severely interference from F^- and AcO^- . In these connections and in continuation to our earlier research [41], we have reported here two novel reversible chromogenic chemosensors L_1 and L_2 containing hydrogen donor for the detection of CN^- in 2:1 CH_3CN-H_2O mixture. Interactions of L_1 and L_2 with CN^- provide remarkable color change from yellow to red (for L_1) and yellow to pink (for L_2).

2. Experimental

2.1. General information

Melting points were determined on an X-4 digital melting-point apparatus and not corrected. UV–Visible spectra were recorded on a Shimadzu UV 1800 spectrophotometer using a 10 mm path length quartz cuvette. 1H NMR spectra of ligand L_1 and L_2 were recorded on a Bruker Ultra shield 200 using $CDCl_3$ at room temperature and NMR titrations were carried out dissolving L_1 and L_2 in DMSO d_6 and cyanide salts in D_2O . The chemical shifts are reported in δ values (ppm) relative to TMS. High resolution mass (HRMS) spectra were recorded on a Waters mass spectrometer using mixed solvent HPLC methanol and triple distilled water. All the chemicals and metal salts were purchased from Merck and the counter ion was used as nitrate for metal and sodium for anions.

2.2. Synthesis and characterization of the probe L_1

To 25 mL of an anhydrous methanol solution of benzil (0.420 g, 2 mmol), 2,4-(dinitrophenyl)hydrazine (0.396 g, 2 mmol) was added. The resulting pale yellow mixture was refluxed for 6 h, under dry condition. Then it was slowly cooled to room temperature. Yellow crystalline solid separated out, which was filtered off and dried in air. Yield, 0.546 g (70%); mp 178 °C Anal. found (calc. for $C_{20}H_{14}N_4O_5$): C, 61.54 (61.53%); H, 3.62 (3.61%); N, 14.35 (14.33%). EI-MS: m/z 390.10 (M^+ , 100%) (Fig. S1). FTIR/ cm^{-1} (KBr): 3441(br), 3269(m), 3112 (w), 2926(w), 1657(w) ($>C=O$), 1621(vs) ($C=N$), 1592(s), 1506(s), 1413(m), 1342(s), 1306(s), 1227(m), 1012(m), 940(w), 840(w), 747(w), 589(w) (Fig. S2). 1H NMR (200 MHz, $CDCl_3$, TMS): δ 11.91 (s, 1H), 9.08 (s, 1H), 8.41 (d, 1H), 8.21 (d, 1H), 7.94 (d, 2H), 7.69 (m, 3H), 7.42–7.51 (m, 2H) (Fig. S3). ^{13}C NMR (200 MHz, $CDCl_3$, TMS): δ 194.27, 151.42, 144.62, 139.07, 135.53, 134.57, 130.81, 129.86, 129.43, 129.02, 127.21, 123.75, 123.21, 116.57, 115.25 (Fig. S4). UV–VIS λ_{max}/nm ($\epsilon/dm^3 mol^{-1} cm^{-1}$)(CH_3CN): 374 (45,600).

2.3. Synthesis and characterization of the probe L_2

For the synthesis of the probe L_2 , the azo dye 2-(4-nitrophenyl)diazonyl-2-hydroxybenzaldehyde (**1**) was prepared first by the following way.

The diazonium salts from aniline derivatives were prepared in good yield according to the previously described methods [42] with slight modification. After completion of diazotization reaction, in a second flask, salicylaldehyde was dissolved in water containing sodium hydroxide and sodium carbonate and cooled to 0 °C in an ice bath. The diazonium solution was slowly added to the phenolate solution in basic medium by adjusting the pH at 7.5–8.5 over 30–45 min. The resulting solution was stirred for 1–2 h in an ice bath and then allowed to reach room temperature to obtain a precipitate. The precipitate was collected and was washed several times with cool water after acidified of the solution (pH =

5.5–6.5) by addition of diluted HCl. The precipitate was finally recrystallized in MeOH/ H_2O to obtain the pure product.

To 25 mL of an anhydrous methanol solution of benzildihydrazone (0.238 g, 1 mmol), the azo dye, 2-(4-nitrophenyl)diazonyl-2-hydroxybenzaldehyde (**1**, 0.542 g, 2 mmol) was added. The resulting yellow mixture was refluxed for 6 h, under dry condition. Then it was slowly cooled to room temperature. Yellow crystalline solid separated out, which was filtered off and dried in air. Yield, 0.543 g (73%); mp > 200 °C Anal. found (calc. for $C_{40}H_{28}N_{10}O_6$): C, 64.50 (64.52%); H, 3.75 (3.79%); N, 18.85 (18.81%). HRMS: 744.22 (M , 100%) (Fig. S5). FTIR/ cm^{-1} (KBr): 3444(br), 3059(w,br), 1614(vs) ($C=N$), 1516 (vs), 1317(vs), 1344(m), 1279(m), 1116(m), 860(m), 689(w) (Fig. S6). 1H NMR (200 MHz, $CDCl_3$, TMS): δ 11.58 (s, 2H) 8.91 (s, 2H), 8.35 (m, 5H), 7.94–8.00 (m, 12H), 7.49 (m, 5H), 6.99 (s, 2H) (Fig. S7). UV–VIS: λ_{max}/nm ($\epsilon/dm^3 mol^{-1} cm^{-1}$)(CH_3CN): 314 (37 800); 374 (44 450).

2.4. UV–Vis titrations

The chemosensors L_1 (3.90 mg, 0.01 mmol) and L_2 (7.44 mg, 0.01 mmol) were dissolved in acetonitrile-water solvent mixture (2:1, v/v, 10 mL) and 30 μ L of them were diluted to 3 mL with the solvent mixture to make a final concentration of 10 μ M. Sodium cyanide (0.1 mmol) was dissolved in 10 mL of triple distilled water and 1.5–90 μ L of the anions solution (10 mM) were transferred to the solutions of L_1 and L_2 (10 μ M) prepared above. After mixing them for a few seconds, UV–Vis spectra were obtained at room temperature.

2.5. Colorimetric test kit

Chemosensors L_1 (3.90 mg, 0.01 mmol) and L_2 (7.44 mg, 0.01 mmol) were dissolved in acetonitrile-water solvent mixture (2:1, v/v) (10 mL) to get 1 mM solution. Test kits were prepared by immersing filter-papers into these solutions (1 mM), and then dried in air to get rid of the solvent. CN^- and different anions (OAc^- , F^- , Cl^- , Br^- , I^- , $H_2PO_4^-$, NO_2^- , NO_3^- , HSO_4^- , N_3^- , CO_3^{2-} , PO_4^{3-} , S^{2-} , and BO_3^{3-} ; 0.001 mmol) were dissolved in acetonitrile-water solvent mixture (2:1, v/v, 10 mL) to prepare 0.1 mM solution. The test kits prepared above were dipped into above-mentioned acetonitrile-water mixture (2:1, v/v) of cyanide ion and other anions and then dried at room temperature.

2.6. Computational details

The GAUSSIAN-09 Revision C.01 program package was used for all calculations [43]. The gas phase geometries of the compound was fully optimized without any symmetry restrictions in singlet ground state with the gradient-corrected DFT level coupled with the hybrid exchange-correlation functional that uses Coulomb-attenuating method B3LYP [44]. Basis set 6-31++G was found to be suitable for the whole molecule.

3. Results and discussion

3.1. Synthesis and structures of L_1 and L_2

Receptor L_1 was obtained in good yield (70%) by the 1:1 condensation reaction of benzil and 2,4-(dinitrophenyl) hydrazone in anhydrous methanol, whereas the receptor L_2 was prepared by the 1:2 condensation reaction of the azo dye 2-(4-nitrophenyl)diazonyl-2-hydroxybenzaldehyde and benzildihydrazone. Both the probes were characterized by 1H NMR, IR and HRMS spectrometry and elemental analyses. Optimized geometries and surface plots of

the chromophores **L**₁ and **L**₂ and their deprotonated species **L**₁-H⁺ and **L**₂-2H⁺ are shown in Figs. 1 and 2 respectively.

3.2. Colorimetric and UV-vis spectral studies

In order to determine the solvatochromic behavior of the synthesized chemosensors, we have recorded the absorption spectra **L**₁ and **L**₂ in different solvents (Figs. S8 and S9) with different polarity (Table 1) as the absorption spectra of the colorant materials in solution depend strongly on the solvent nature and solvent-solute interactions. With increase in solvent polarity, maximum absorption band (λ_{max}) of the chemosensors **L**₁ and **L**₂ showed bathochromic shifts (positive solvatochromism). The new absorption bands at higher wavelengths are due to the interaction at the H-atoms of amine moiety in **L**₁ and of hydroxyl group of the chemosensor **L**₂, in relatively basic solvent DMSO. These results suggest that in polar solvents, the ground states of the tested chemosensors **L**₁ and **L**₂ are better stabilized relative to the excited state. For this reason, moderate polar solvent acetonitrile was selected as the best solvent for the colorimetric sensing of chemosensors **L**₁ and **L**₂.

In order to investigate the selectivity of the probes **L**₁ and **L**₂ colorimetrically towards various anions such as OAc⁻, F⁻, Cl⁻, Br⁻, I⁻, H₂PO₄⁻, NO₂⁻, NO₃⁻, HSO₄⁻, N₃⁻, CO₃²⁻, PO₄³⁻, S²⁻, and BO₃³⁻, visual detection was carried out in 2:1 (v/v) CH₃CN-H₂O mixture. As it is observed by the naked eye, **L**₁ and **L**₂ showed a remarkable color change from yellow to red for **L**₁ and yellow to pink for **L**₂ upon the addition of 10 equiv. of CN⁻ ions (Fig. 3). In contrast, the other

metal ions did not show any significant color change. These indicate that the probes **L**₁ and **L**₂ can serve as 'naked-eye' cyanide indicators. The spectral responses were also investigated upon addition of 10 equiv. of various anions to **L**₁ and **L**₂ (2×10^{-5} M) solution in acetonitrile-water (2:1, v/v) mixture (Fig. 4). Absorption spectra of free receptors **L**₁ and **L**₂ in acetonitrile water (2:1, v/v) mixture exhibited same absorption band 374 nm. A large bathochromic shift ($\Delta\lambda_{\text{max}}$) of 136 nm was observed in the absorption spectra for **L**₁ in the presence of CN⁻ ions whereas for ($\Delta\lambda_{\text{max}}$) of 129 nm was observed in the absorption spectra for **L**₂ in the presence of CN⁻ ions. In Fig. S10 of Supporting Information, bar graphs showing the relative absorption intensities of **L**₁ and **L**₂ upon treatment with various anions have been given.

The large bathochromic shifts were attributed due to the deprotonation of the -NH proton and -OH proton (from **L**₁ and **L**₂ respectively) by the CN⁻ ion and as a result of which the electron density on nitrogen and oxygen atoms are increased and the electrons are rearranged in the whole molecule leading to the more stable delocalized structures. Moreover due to the presence of chromophoric azo group (N=N) and the electron-deficient -NO₂ group, intramolecular charge transfer (ICT) processes become more efficient. The other anions cannot show any significant absorption band shift as well as color change indicating no such deprotonation.

In order to determine the sensitivities of **L**₁ and **L**₂ towards CN⁻ ion, we have carried out UV-vis spectrophotometric titrations by adding a standard solution of CN⁻ as their sodium salts to the

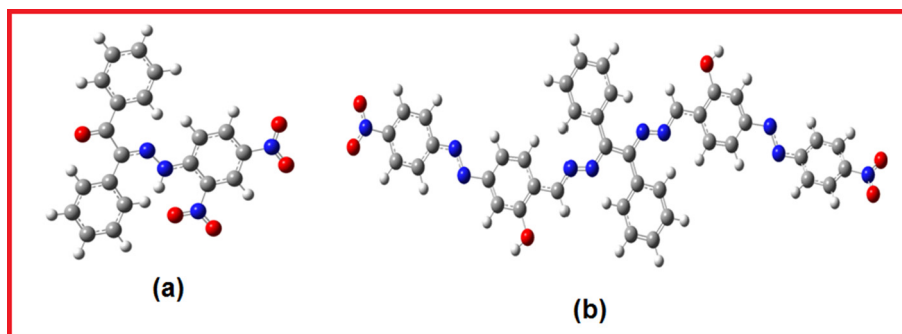


Fig. 1. Geometry optimized diagrams of the molecules (a) **L**₁ and (b) **L**₂.

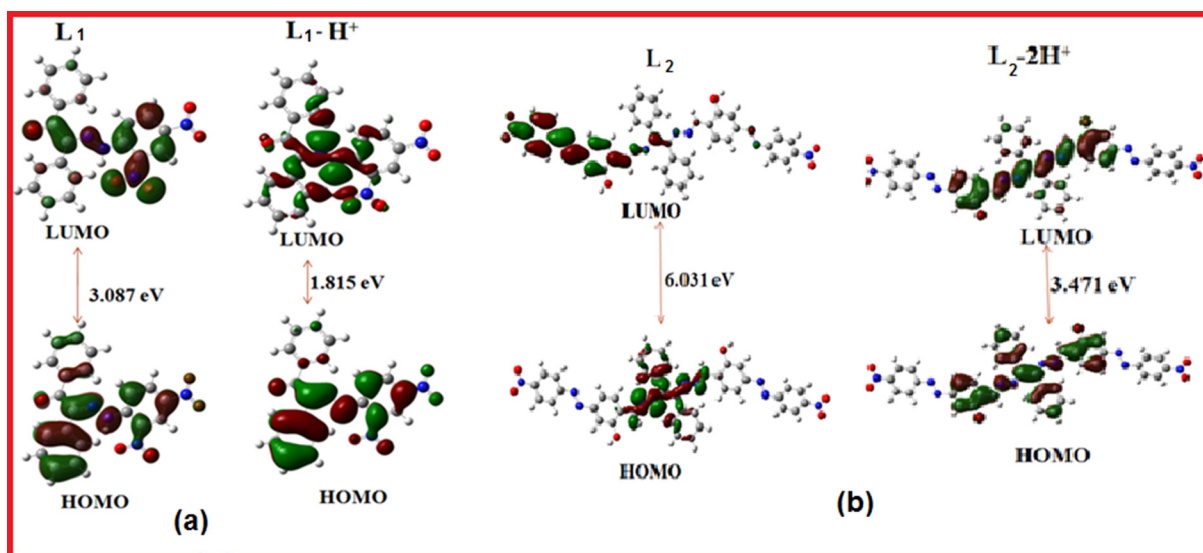


Fig. 2. Surface plots of HOMO and LUMO of (a) **L**₁ and **L**₁-H⁺; (b) **L**₂ and **L**₂-2H⁺ with their energy differences.

Table 1
Absorption properties of **L**₁ and **L**₂ in various solvents.

Solvent	λ_{\max} (nm) for L ₁	λ_{\max} (nm) for L ₂
Methanol	378	369
Chloroform	372	378
Acetonitrile	374	374
DMSO	393, 525	571
<i>n</i> -Hexane	355	–

CH₃CN-H₂O (2:1, v/v) solution of **L**₁ and **L**₂ (2.25×10^{-5} M) (Fig. 5). On the treatment of CN⁻ ions, the intensity of absorption band at 374 nm decreased significantly for both the ligand **L**₁ and **L**₂, and new absorption bands at 510 and 503 nm appeared respectively for **L**₁ and **L**₂, on the addition of 10 equiv. of CN⁻ ion. Clear isosbestic points were observed at 435 and 408 nm for **L**₁ and **L**₂ indi-

cating single product was formed after the addition of CN⁻ in each case.

From the above titration experiments of **L**₁ and **L**₂, ratiometric calibration curves have been determined, as it is essential to increase dynamical behaviors of the chemosensors towards cyanide detection. The curves show linear dependence of the ratio of the absorbances at 510 nm and 374 nm (A₅₁₀/A₃₇₄) for **L**₁ and 505 nm and 374 nm (A₅₀₅/A₃₇₄) for **L**₂ as function of CN⁻ concentration (Fig. S11, Supporting Information), which enables ratiometric quantification of CN⁻. Good linearity was observed in the range of 0–1.2 mM. From these calibration curves detection limit can be calculated based on the formula $3SD/m$ where SD is the standard deviation of the blank solution and 'm' is the slope of the calibration curve. The calculated values of detection limit are 1.3 μ M for **L**₁ and 1.0 μ M for **L**₂. These values are lower than the permissible limit (1.9 μ M) in drinking water set by the WHO.



(a)



Fig. 3. Color changes of (a) **L**₁ and (b) **L**₂ after addition of 10 equiv. of different anions in CH₃CN-H₂O (2:1, v/v) mixture.

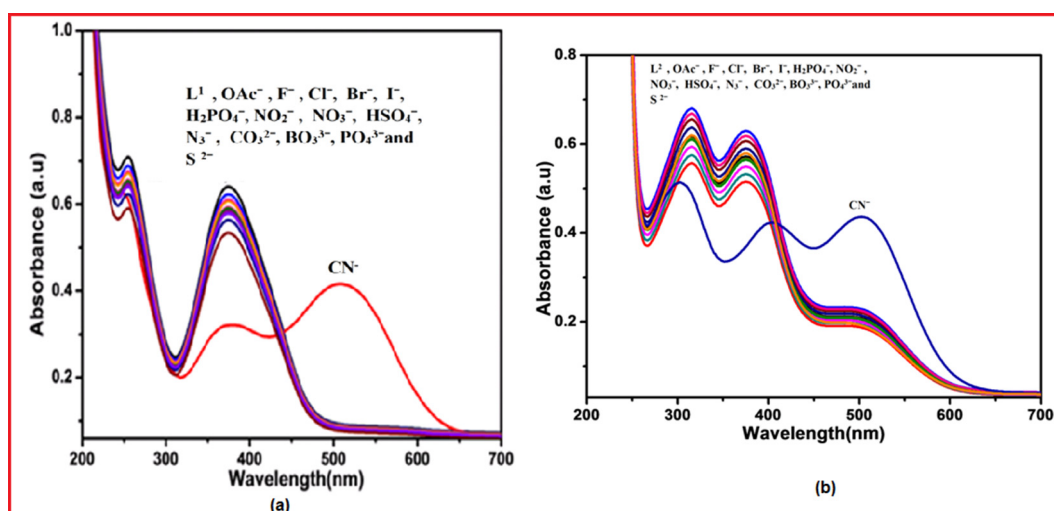


Fig. 4. UV-vis spectral responses of (a) **L**₁ and (b) **L**₂ (2.25×10^{-5} M) before and after addition of 10 equiv. of different anions in CH₃CN-H₂O (2:1, v/v) mixture.

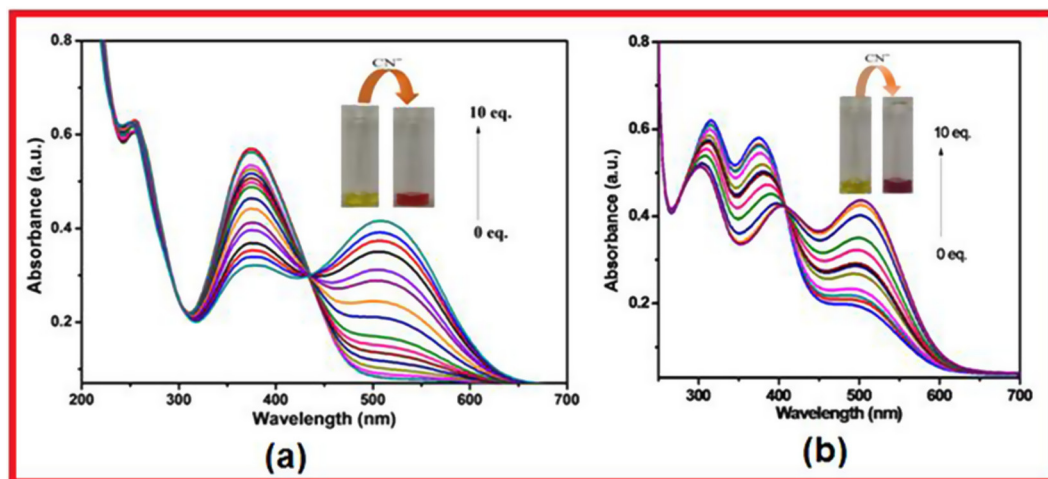


Fig. 5. UV-vis titration of **L** with cyanide ion (0–10 equiv.) in $\text{CH}_3\text{CN-H}_2\text{O}$ (2:1, v/v) solution.

To determine the binding selectivity of CN^- ion towards **L**₁ and **L**₂ in presence of other interfering ions the UV-visible spectra were studied in the presence of various competing anions such as OAc^- , F^- , Cl^- , Br^- , I^- , H_2PO_4^- , NO_2^- , NO_3^- , HSO_4^- , N_3^- , CO_3^{2-} , PO_4^{3-} , S^{2-} , and BO_3^{3-} . For competition tests, receptors **L**₁ and **L**₂ were treated with 5 equiv. of CN^- in the presence of 6 equiv. of other anions. No interference was observed for the detection of CN^- in the presence of other anions (Fig. S12, Supporting Information). This result indicates that the chemosensors **L**₁ and **L**₂ have excellent selectivity towards CN^- in presence of competing ions even OAc^- , F^- and H_2PO_4^- ions.

In order to determine the binding stereochemistry of **L**₁ and **L**₂ towards cyanide ion Job's continuous variation method was used. For the probe **L**₁ absorption band of wavelength 510 nm reaches maximum intensity when mole fraction of cyanide ion within the range of 0.45–0.55, indicating that the receptor **L**₁ binds to CN^- ions in a 1:1 [**L**₁: CN^-] ratio (Fig. S13, Supporting Information). But in the case of **L**₂, absorption band of wavelength 505 nm reaches maximum intensity when mole fraction of cyanide ion at around 0.38, indicating that the receptor binds to CN^- ions in a 1:2 [**L**₂: CN^-] ratio (Fig. S14, Supporting Information).

From UV-Vis spectral change, the binding constants for the formation of the respective complexes were evaluated using the Benesi-Hildebrand (B-H) plot, Eq. (1).

$$1/(A - A_0) = 1/\{K(A_{\text{max}} - A_0)[\text{C}]^n\} + 1/(A_{\text{max}} - A_0) \quad (1)$$

where A_0 is the absorbance of free receptor **L**₁/**L**₂ at particular wavelength, and A is the observed absorbance at that wavelength in any intermediate metal ion concentration (C). A_{max} is the absorbance intensity value that was obtained in presence of anion at saturation.

Assuming 1:1 stoichiometry for **L**₁- CN^- adduct, binding constant (K) has been determined from the intercept of the linear plot (Fig. S15a, Supporting Information). Considering 1:2 stoichiometry for **L**₂- CN^- adduct, binding constant (K) has also been determined from the intercept of the linear plot (Fig. S15b, Supporting Information). The free energy changes of complex formation reactions have been determined using the relation, $\Delta G = -RT \ln K$ (Table 2). Higher the value of negative free energy, stron-

Table 2
Calculated thermodynamic parameters for **L**- CN^- (where **L** = **L**₁ and **L**₂).

Chemosensor	Binding const. (K) (M^{-1})	Free energy ($-\Delta G$) (kJ/mole)
L ₁	1.71×10^5	2.91×10^4
L ₂	2.77×10^{11}	6.52×10^4

ger interaction is present between host and guest, which shifted the maximum absorption band towards higher wavelength.

3.3. pH and time dependence

The pH dependence of **L**₁ and **L**₂ were checked by UV-vis spectroscopy using 100 mM HEPES buffer. No significant change occurred in pH less than 6 for both **L**₁ and **L**₂ probably due to hydrolysis of imine linkage. As the pH raises (pH = 7–8), the intensity of the absorption band at ~500 nm increases; this is due to an increase in the hydroxyl ions concentration which interacts with the $-\text{NH}$ and $-\text{OH}$ protons of the chemosensors **L**₁ and **L**₂. It was also observed that, the interaction of chemosensors with the amine or hydroxyl proton occurred effectively at pH values higher than 8 (Fig. S16, Supporting Information). This effect has been attributed to the de-protonating of amine and phenolic group of the probes in highly basic conditions. These findings indicated that the synthesized chemosensors were sensitive to the pH values, and can be used any pH range from 6 to 12.

The time evolution of the receptors **L**₁ and **L**₂ in the presence of 5 equiv. of CN^- ion in $\text{CH}_3\text{CN-H}_2\text{O}$ (2:1 v/v) were also investigated. The recognition interactions get almost completed just after the addition of 5 equiv. of CN^- ion and the absorbance intensity remains almost the same up to 15 min. This ensures that the receptor **L**₁ and **L**₂ to be a sensitive sensor.

3.4. Reversibility test

To examine the reversibility of the receptors **L**₁ and **L**₂ towards CN^- ion we have added hydrochloric acid (HCl, 5 equiv.) to the guest adduct **L**- CN^- (Fig. 6). The red and pink color solution of **L**₁- CN^- and **L**₂- CN^- adducts reappear to original host yellow color after addition of HCl solution along with the disappearance of red shifted band at 510 and 505 nm for **L**₁ and **L**₂. Upon addition of excess CN^- into the solution again, the color and the absorbance were recovered. The color changes were almost reversible even after several cycles with the sequentially alternative addition of CN^- and HCl. These results indicate that receptors **L**₁ and **L**₂ could be recyclable than any irreversible base catalysed reaction and further confirm that both the probes **L**₁ and **L**₂ would detect CN^- by the deprotonation mechanism.

In order to be confirmed whether the color and spectral changes initiated from the ICT mechanism through the de-protonation of $-\text{NH}$ and $-\text{OH}$ moiety and the interactions between chemosensors **L**₁ and **L**₂ and OH^- were also conducted. The color and UV-vis

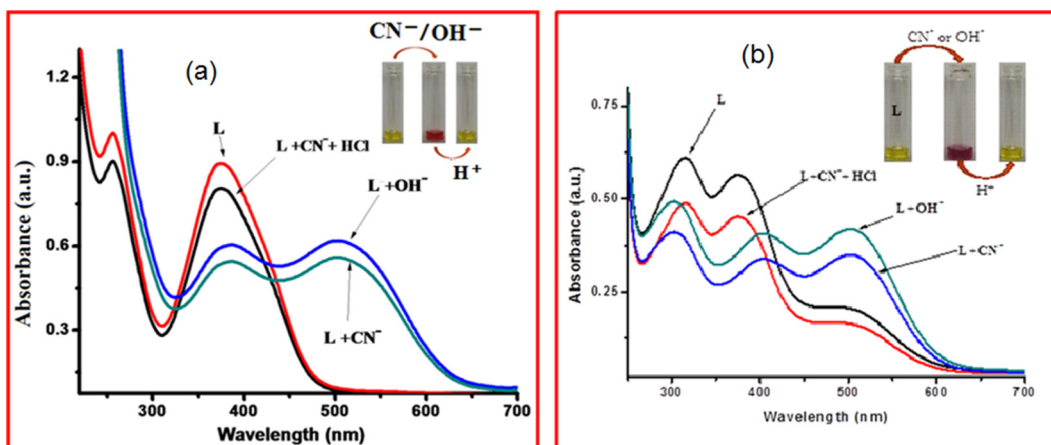


Fig. 6. Change of absorbance spectra of (a) L_1 and (b) L_2 on alternate addition of CN^- and HCl.

spectral change of the probes L_1 and L_2 upon addition of OH^- were nearly identical to those of addition of CN^- except slightly less intensity, which support the deprotonation mechanism of L by CN^- ion, which have further been supported by HRMS studies. In HRMS, the peak around 389 was assignable to L_1-H^+ (Fig. S17 of Supporting Information) and the peak around 742 was assignable to L_2-2H^+ (Fig. S18, Supporting Information). The de-protonation mechanism has also been verified by the DFT study of the L_1-H^+ and L_2-2H^+ species. The HOMO-LUMO energy in L_1-H^+ (1.815 eV) and L_2-2H^+ (3.471 eV) are much lower than that in free L_1 (3.087 eV) and L_2 (6.031 eV) (shown in Fig. 2).

3.5. Sensing mechanism

In order to study the nature of the interactions between the chemosensors L_1 and L_2 with CN^- ion, 1H NMR experiments have been conducted. Fig. S19a of Supporting Information shows the 1H NMR spectra of L_1 in the absence and presence of 1.5 equiv. of CN^- ion (in DMSO d_6 and D_2O mixture). It is clear from the 1H NMR spectra that the addition of 1.5 equiv. of CN^- results in the disappearance of the proton signal at δ 11.91 ($-NH$ proton). From Fig. S19b it can also be seen that on the addition of 2.5 equiv. of CN^- the proton signal at δ 11.58 ($-OH$ proton) disappeared. Moreover, the other aromatic protons are shifted slightly towards up field for both the cases (Fig. S19, Supporting Information).

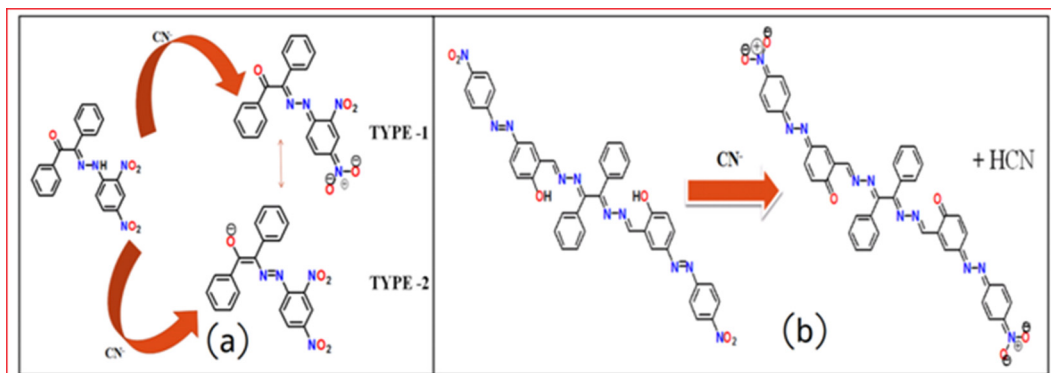
To further investigate the interactions between the probes L_1 and L_2 and CN^- ions, the infrared spectra of L and $L-CN^-$ adduct were compared. As shown in Fig. 20a of Supporting Information, the stretching vibration peaks at 3441 cm^{-1} ($-NH$) of chemosensor

L_1 completely disappeared after the addition of 1.5 equiv of CN^- ion to the probe L_1 . The other sharp IR peaks become broad due to delocalization effect of whole molecule which demonstrates that chemosensor L_1 reacted with CN^- ion. For L_2 , addition of 2.5 equiv. of CN^- ion to the probe the stretching vibration peaks at 3444 cm^{-1} ($-OH$) of chemosensor L_2 also completely disappeared (Fig. S20b, Supporting Information). Therefore, these results of 1H NMR experiments and IR studies validate the de-protonation of amine group and hydroxyl group during the anion recognition process as shown in Scheme 1.

The chemosensors L_1 and L_2 contain azo groups and electron-withdrawing $-NO_2$ groups, which increase the acidity as well as the H-bond donating ability of the H-atom of the $-NH/-OH$ moiety towards suitable anions. In the aqueous solution of anions, H_2O itself compete with the anions for the binding sites of receptor and therefore, could disturb hydrogen bonding interactions between CN^- and the receptor. Additionally there is a red shifted band above 500 nm of the receptors L_1 and L_2 in basic solvent DMSO which has less capacity to participate in H-bond formation. Thus deprotonation predominant over H-bonding interaction; which is also confirmed by NMR and IR studies. The pK_a value supports the selectivity of CN^- ion over competing ion F^- , OAc^- and $H_2PO_4^-$ ions in aqueous solution. The pK_a value of the two ligands L_1 and L_2 have been obtained by the pH-dependent UV-vis spectra using the following Eq. (2)

$$pK_a = pH - \log\left[\frac{(A_{acidic} - A_{int})}{(A_{int} - A_{basic})}\right] \quad (2)$$

where, A_{acidic} is the absorbance in acidic condition, A_{int} is the intermediate absorbance (absorbance at pH at 7) and A_{basic} is the



Scheme 1. Proposed sensing mechanism of (a) L_1 and (b) L_2 .

Table 3
Determination of cyanide in different water samples using **L**₁.

Samples	Added (μM)	Found (μM)	Recovery (%)	RSD ^a (%)
Tap water	10	10.9	109	2.1
	20	19.7	98	1.5
Rain water	10	11.7	117	1.8
	20	21.2	106	2.7
Simulated urine sample	10	9.3	93	2.2
	20	19.1	95	1.3

^a Three independent measurements.

absorbance in basic condition. We considered A_{acidic} in the absorbance at pH = 6 (because of the fact that at lower pH the imine bonds of the Schiff bases **L**₁ and **L**₂ may break) and A_{basic} absorbance at pH at 10. Calculated pK_a values of the ligands **L**₁ and **L**₂ are 8.30 and 8.18 respectively. The pK_a value of HCN in water (9.30) is much higher than that of other acids (pK_a = 4.75 and 3.17 for HOAc and HF in water respectively) and those of the chemosensors **L**₁ and **L**₂. Solvation of F⁻ and OAc⁻ in water is high for small size and small radius. As a result their basicity is decreased; they cannot show any competition with CN⁻ ions. CN⁻ ion has less solvation in water, so the weaker H-bonding ability in comparison with F⁻ and AcO⁻, which also favours the deprotonation in the probes **L**₁ and **L**₂ and therefore result in high selectivity for cyanide ion.

3.6. Colorimetric test kit

To check the practical application, the test kits were utilized to sense cyanide ion among different anions. As shown in Fig. S21 of Supporting Information, when the test kits coated with **L**₁ or **L**₂ were added to different anions solutions, the obvious color change was observed only with CN⁻ ions in CH₃CN-H₂O (2:1, v/v) mixture. Therefore, the test kits coated with the chemosensors **L**₁ and **L**₂ solution would be convenient for detecting CN⁻ ions. These results showed that the probes **L**₁ and **L**₂ could be a valuable practical sensor for environmental analyses of CN⁻ ions.

3.7. Real sample analysis

Designing a sensor is getting fulfilled only when it will be useful in practical applications. Sensing cyanide in drinking water and tap water were demonstrated with the probes **L**₁ and **L**₂. In order to evaluate the practical feasibility, the **L**₁ and **L**₂ were used for the determination of CN⁻ ions in different water samples collected from tap and rain water and simulated urine samples. The spiked cyanide concentrations were of 10 and 20 μM. The determined concentrations for **L**₁ are: tap water (10.8 and 19.8 μM); rain water (11.7 and 21.5 μM) and simulated urine sample (9.4 and 19.2). The corresponding recoveries are: tap water (108% and 99%); rain water (117% and 107%) and urine sample (94% and 96%) (Table 3). Appreciable recoveries also achieved by using the probe **L**₂, in the determination of cyanide ion in various water samples and simulated urine samples. These results revealed good practical feasibility of the chemosensors **L**₁ and **L**₂ in quantitative estimation of cyanide ion in different environmental and biological samples (Table 3).

4. Conclusion

In this work simple, sensitive and useful method for colorimetric detection and determination of CN⁻ ions using novel hydrazone based N, O donor Schiff-bases **L**₁ and **L**₂ have been described. The colorimetric properties of the synthesized chemosensors **L**₁ and

L₂ towards various anions were tested visually and with UV-vis absorption spectrometry. The probes **L**₁ and **L**₂ are having two strong electron withdrawing groups (-NO₂) and showed remarkable color change from yellow to red (for **L**₁) and yellow to pink (for **L**₂) upon addition of CN⁻ ion in acetonitrile-water (2:1, v/v) solution. The detection limits reach up to 1.3 μM for **L**₁ and 1.0 μM for **L**₂, far lower than the WHO permissible limit. The solvatochromic behaviors of the chemosensors **L**₁ and **L**₂ revealed that there are large bathochromic shifts upon increasing solvent polarity and pH values. The sensing mechanisms have been confirmed by ¹H NMR experiments, HRMS and IR analysis as well as DFT studies. **L**₁ and **L**₂ can be successfully applied for the determination of CN⁻ ion in real samples.

Acknowledgements

G.K.P would like to thank the Department of Science and Technology and Department of Biotechnology, Government of India, New Delhi for financial support.

Appendix A. Supplementary data

Supplementary data associated with this article can be found, in the online version, at <https://doi.org/10.1016/j.ica.2018.01.013>.

References

- [1] D. Chen, R.J. Letcher, L.T. Gauthier, S.G. Chu, R. McCrindle, D. Potter, *Environ. Sci. Technol.* 45 (2011) 9523–9530.
- [2] (a) Q. Wang, Y. Xie, Y. Ding, X. Li, W. Zhu, *Chem. Commun.* 46 (2010) 3669–3671; (b) Y. Ding, T. Li, W. Zhuand, Y. Xie, *Org. Biomol. Chem.* 10 (2012) 4201–4207.
- [3] C.R. Wang, Q.B. Lu, *J. Am. Chem. Soc.* 132 (2010) 14710–14713.
- [4] Y. Kim, H. Kwak, S.J. Lee, J.S. Lee, H.J. Kwon, S.H. Nam, K. Lee, C. Kim, *Tetrahedron* 62 (2006) 9635–9640.
- [5] J.J. Park, Y. Kim, C. Kim, J. Kang, *Tetrahedron Lett.* 52 (2011) 2759–2763.
- [6] B. Vennesland, E.E. Comm, C.J. Knowlles, J. Westly, F. Wissing, *Cyanide in Biology*, Academic Press, London, 1981.
- [7] J.Y. Noh, I.H. Hwang, H. Kim, E.J. Song, K.B. Kim, C. Kim, *Bull. Korean Chem. Soc.* 34 (2013) 1985–1989.
- [8] G.J. Park, I.H. Hwang, E.J. Song, H. Kim, C. Kim, *Tetrahedron* 70 (2014) 2822–2828.
- [9] L. Tang, P. Zhou, K. Zhong, S. Hou, *Sens. Actuators, B* 182 (2013) 439–445.
- [10] R. Yang, W. Wu, W. Wang, Z. Li, J. Qin, *Macromol. Chem. Phys.* 211 (2010) 18–26.
- [11] B. Chen, Y. Ding, X. Li, W. Zhu, J.P. Hill, K. Ariga, Y. Xie, *Chem. Commun.* 49 (2013) 10136–10138.
- [12] (a) Y. Xie, Y. Ding, X. Li, C. Wang, J.P. Hill, K. Ariga, W. Zhanga, W. Zhu, *Chem. Commun.* 48 (2012) 11513–11515; (b) X. Chen, S. Nam, G. Kim, N. Song, Y. Jeong, I. Shin, S.K. Kim, J. Kim, S. Park, J. Yoon, *Chem. Commun.* 46 (2010) 8953–8955.
- [13] Y. Qu, B. Jin, Y. Liu, Y. Wu, L. Yang, J. Wu, J. Hu, *Tetrahedron Lett.* 54 (2013) 4942–4944.
- [14] (a) S. Sumiya, T. Doi, Y. Shiraishi, T. Hirai, *Tetrahedron* 68 (2012) 690–696; (b) V.K. Gupta, A.K. Singh, N. Gupta, *Sens. Actuators, B* 204 (2014) 125–135; (c) S.S. Razi, R. Ali, P. Srivastava, A. Misra, *Tetrahedron Lett.* 55 (2014) 2936–2941; (d) M. Kumar, R. Kumar, V. Bhalla, *Tetrahedron Lett.* 54 (2013) 1524–1527.
- [15] S.A. Lee, G.R. You, Y.W. Choi, H.Y. Jo, A.R. Kim, I. Noh, S. Kim, Y. Kim, C. Kim, *Dalton Trans.* 43 (2014) 6650–6659.
- [16] C. Young, L. Tidwell, C. Anderson, *Cyanide: Social, Industrial and Economic Aspects: Minerals, Metals and Materials Society*, Warrendale, 2001.
- [17] K.B. Kim, H. Kim, E.J. Song, S. Kim, I. Noh, C. Kim, *Dalton Trans.* 42 (2013) 16569–16577.
- [18] (a) J. Xu, K. Liu, D. Di, S. Shao, Y. Guo, *Inorg. Chem. Commun.* 10 (2007) 681–684; (b) C. Suksai, T. Tuntulani, *Chem. Soc. Rev.* 32 (2003) 192–202.
- [19] (a) S.L. Wiskur, H. Aithaddou, J.V. Lavigne, E. Anslyn, *Acc. Chem. Res.* 34 (2001) 963–972; (b) H.G. Loehr, F. Vogtle, *Acc. Chem. Res.* 18 (1985) 65–72.
- [20] (a) Y. Sun, Y.L. Liu, W. Guo, *Sens. Actuator B Chem.* 143 (2009) 171–176; (b) Z. Xu, X. Chen, H.N. Kim, J. Yoon, *Chem. Soc. Rev.* 39 (2010) 127–137.
- [21] K. Lee, H. Kim, G. Kim, I. Shin, J. Hong, *Org. Lett.* 10 (2008) 49–51.
- [22] J.P. Anzenbacher, A.C. Try, H. Miyajii, K. Jursikova, V.M. Lynch, M. Marquez, J.L. Sessler, *J. Am. Chem. Soc.* 122 (2000) 10268–10269.
- [23] H. Miyajii, W. Sato, J.L. Sessler, *Angew. Chem., Int. Ed.* 39 (2000) 1777–1780.
- [24] L. Zhou, H. Sun, H. Li, H. Wang, X. Zhang, S. Wu, S. Lee, *Org. Lett.* 6 (2004) 1071–1074.

- [25] J. Yoshino, N. Kano, T. Kawashima, *J. Org. Chem.* 74 (2009) 7496–7498.
- [26] K.P. Divya, S. Sreejith, B. Balakrishna, P. Jayamurthy, P. Anees, A. Ajayaghosh, *Chem. Commun.* 46 (2010) 6069–6071.
- [27] J.Y. Park, Y. Hirata, K. Hamada, *Dyes Pigm.* 95 (2012) 502–511.
- [28] A. Mohammadi, B. Khalili, M. Tahavor, *Spectrochim. Acta A* 150 (2015) 799–804.
- [29] D.H. Song, H.Y. Yoo, J.P. Kim, *Dyes & Pigm.* 75 (2007) 727–731.
- [30] F. Chami, M.R. Wilson, *J. Am. Chem. Soc.* 132 (2010) 7794–7795.
- [31] W. Huang, Y. Li, H. Lin, *Spectrochim. Acta A* 86 (2012) 437–443.
- [32] N. Hosain-Nataj, E. Mohajerani, H. Nemati, A. Moheghi, M.R. Yazdanbakhsh, M. Goli, A. Mohammadi, *J. Appl. Polym. Sci.* 127 (2013) 456–462.
- [33] Y. Xia, C. Fan, B. Zhao, J. Zhao, D. Shin, J. Miao, *Eur. J. Med. Chem.* 43 (2008) 2347–2353.
- [34] S.N. Pandeya, D. Sriram, G. Nath, E. DeClercq, *Eur. J. Pharm. Sci.* 9 (1999) 25–31.
- [35] V. Thiagarajan, P. Ramamurthy, D. Thirumalai, V.T. Ramakrishnan, *Org. Lett.* 7 (2005) 657–660.
- [36] L. Pei, Q. Lin, H. Chao, L. Ji, *Inorg. Chem. Commun.* 22 (2012) 90–92.
- [37] S.S. Razi, R. Ali, P. Srivastava, M. Shahi, A. Misra, *RSC Adv.* 4 (2014) 16999–17007.
- [38] N. Mergu, V.K. Gupta, *Sens. Actuators B* 210 (2015) 408–413.
- [39] R. Kumar, V. Bhalla, M. Kumar, *Dalton Trans.* 42 (2013) 8808–8814.
- [40] D. Wang, J.Q. Zheng, X. Yan, X.J. Zheng, L.P. Jin, *RSC Adv.* 5 (2015) 64756–64762.
- [41] (a) A. Ghorai, J. Mondal, S. Chowdhury, G.K. Patra, *Dalton Trans.* 45 (2016) 11540–11553;
(b) A. Ghorai, J. Mondal, R. Chandra, G.K. Patra, *Dalton Trans.* 44 (2015) 13261–13271;
(c) A. Ghorai, J. Mondal, R. Chandra, G.K. Patra, *RSC Adv.* 6 (2016) 72185–72192.
- [42] T. Hu, I.R. Baxendale, M. Baumann, *Molecules* 21 (2016) 918–930.
- [43] M.J. Frisch, G.W. Trucks, H.B. Schlegel, G.E. Scuseria, M.A. Robb, J.R. Cheeseman, G. Scalmani, V. Barone, B. Mennucci, G.A. Petersson, H. Nakatsuji, M. Caricato, X. Li, H.P. Hratchian, A.F. Izmaylov, J. Bloino, G. Zheng, J.L. Sonnenberg, M. Hada, M. Ehara, K. Toyota, R. Fukuda, J. Hasegawa, M. Ishida, T. Nakajima, Y. Honda, O. Kitao, H. Nakai, T. Vreven, J.A. Montgomery Jr., J.E. Peralta, F. Ogliaro, M. Bearpark, J.J. Heyd, E. Brothers, K.N. Kudin, V.N. Staroverov, R. Kobayashi, J. Normand, K. Raghavachari, A. Rendell, J.C. Burant, S.S. Iyengar, J. Tomasi, M. Cossi, N. Rega, J.M. Millam, M. Klene, J.E. Knox, J.B. Cross, V. Bakken, C. Adamo, J. Jaramillo, R. Gomperts, R.E. Stratmann, O. Yazyev, A.J. Austin, R. Cammi, C. Pomelli, J.W. Ochterski, R.L. Martin, K. Morokuma, V.G. Zakrzewski, G.A. Voth, P. Salvador, J.J. Dannenberg, S. Dapprich, A.D. Daniels, Ö. Farkas, J.B. Foresman, J.V. Ortiz, J. Cioslowski, D.J. Fox, *Gaussian 09, Revision C.01*, Gaussian Inc., Wallingford, CT, 2009.
- [44] (a) A.D. Becke, *J. Chem. Phys.* 98 (1993) 5648–5652;
(b) C. Lee, W. Yang, R.G. Parr, *Phys. Rev. Sect. B* 37 (1988) 785–789.